



# American Journal of Innovation in Science and Engineering (AJISE)

ISSN: 2158-7205 (ONLINE)

VOLUME 4 ISSUE 1 (2025)



PUBLISHED BY  
E-PALLI PUBLISHERS, DELAWARE, USA

## Performance Analysis of a Three-Axle Rigid Minecart in The Oil and Gas Suspension System under Variable Conditions

Md Khairul Basher<sup>1</sup>, Md Tariqul Islam<sup>1\*</sup>, Akash Joarder<sup>2</sup>, Md Niaz Ahmed<sup>2</sup>

### Article Information

**Received:** November 12, 2024

**Accepted:** December 20, 2024

**Published:** January 07, 2025

### Keywords

*Cylinder Stress, Hydro-Pneumatic Suspension, Minecart, Mises Stress Analysis*

### ABSTRACT

This research article investigates the nonlinear characteristics of a three-axle rigid mine car equipped with a balanced hydro-pneumatic suspension system and the influential factors affecting these characteristics. Through extensive simulation calculations, the performance of the suspension system was assessed under obstacle-crossing trench conditions. A comprehensive multi-signal data acquisition and analysis system was developed to synchronously collect critical parameters such as pressure displacement within the oil and gas suspension cylinder and stress and strain data from the supporting structure. The resulting time-domain curves captured variations in these parameters during testing at speeds of 10 km/h and 25 km/h on flat surfaces and obstacles with specified dimensions. The interaction between the suspension cylinder's loading capacity and operational characteristics was evaluated, revealing a significant inverse relationship between pressure and displacement, particularly within the front suspension system. Stress analysis indicated high stress concentrations at critical points during obstacle crossings, suggesting areas for potential performance improvements. Additionally, findings demonstrated that maximum stress in the cylinder support occurs during dynamic loading conditions, highlighting the need for reinforced designs under such scenarios. Collectively, this comprehensive analysis lays the groundwork for enhancing the robustness of oil and gas suspension systems in mining vehicles, contributing valuable insights for their future development.

### INTRODUCTION

The development and utilization of mineral resources have become an important pillar of China's social and economic development (Wang *et al.*, 2021). As the main transportation equipment of large-scale open-pit mines, mine trucks are responsible for the mining and transporting of 90% of the world's iron ore and 40% of the world's coal mines (Zhu, 2009). China's non-road mining trucks started relatively late, relying on imports for a long time, and it was not until the 70s of the 20th century that they began to develop independently, and it was not until the 90s that they began to form a scale (Li, 2015). With the rapid economic development of China's neighboring countries and African countries, the development of mineral resources has gradually increased, and the market demand for large mining trucks is increasing day by day. At the same time, the National Standards and Regulations department has gradually improved the technical standards and test methods of mining truck products from the aspects of safety, performance, ergonomics, and reliability, involving mining wide-body vehicles, mining mechanical transmission dump trucks, and mining electric transmission dump trucks, which are used for service product development and certification, making the competition and development of mining trucks enter a new era (Zhang, 2013).

Since the 20th century, the classic two-axle mining dump truck has been unable to meet the demand, Chinese

enterprises broke through the bottleneck, XCMG Group, Sany Group, and Shaanxi Tongli as the representatives of the construction machinery enterprises opened the road of independent research and development developed a class of China's unique three-axle rigid mining truck products, the use of rigid frame structure, oil and gas balance suspension system, combined with the three-axle layout, the application of wide-body vehicle localization support, for product development to save a lot of costs, while increasing the carrying capacity of the minecart, but also has high reliability (Zhang, 2013). To improve the carrying capacity of the minecart, the overall structure size of the vehicle is bound to increase, and the weight of the whole vehicle will also increase, due to the weight difference of the minecart when driving with light load and heavy load 2-3 times, to ensure the driving smoothness and safety, the oil and gas suspension system with high adaptability to working conditions will be selected (Guo, 2021).

Oil and gas suspension technology began in the 60s of the 20th century, which is based on inert gas as the elastic medium, that is, the compression characteristics of the gas are used to realize the role of elastic elements, and then the damping of the liquid flow is used to achieve vibration damping, and the liquid is used as the force transmission medium to realize the transmission of force through the pressure change generated by the liquid load, which is a suspension system integrating elastic elements

<sup>1</sup> China University of Mining and Technology, Xuzhou, Jiangsu, 221116, China

<sup>2</sup> University of Technology Sydney, Sydney, Ultimo NSW 2007, Australia

\* Corresponding author's e-mail: [tariqulislam@cumt.edu.cn](mailto:tariqulislam@cumt.edu.cn)

and vibration damping elements (Fei, 2015; Feng & Wang, 2000). When the vehicle is driving on uneven roads, due to the vibration of the vehicle caused by road surface excitation, the piston rod of the oil and gas suspension system moves up and down. The hydraulic oil flows through the throttle hole to generate throttle damping force. The size of the throttle damping force depends on the throttle area of the throttle hole, and the step-less adjustment of the suspension damping can be realized by changing the aperture of the throttle hole. The inert gas pressure in the air chamber also changes with the movement displacement to produce elastic force, which mainly relies on the throttle damping force and the elastic force of the air chamber to attenuate the vibration of the body (Wu *et al.*, 2020). The stiffness of the oil and gas suspension system depends on the performance parameters of the accumulator, and the suspension damping depends on the size of the orifice, check valve structure, and other factors (Guan *et al.*, 2020). Taking advantage of the easy adjustment of the relative stiffness of the damping, the purpose of active control of the suspension can also be achieved by adjusting the damping size (Yin *et al.*, 2022). Good suspension system performance is crucial to improve the handling stability, driving speed, driving smoothness, structural life, and fuel consumption of the vehicle (Goodall & Kortüm, 1983; Margolis, 1983; Dindarloo, 2016).

In this paper, a typical three-axle rigid minecart is taken as the research object. The characteristics of the vehicle's oil and gas suspension system are studied through simulation

analysis. The output force of the cylinder is analyzed by using the force of the cylinder frame support as the carrier. By building a multi-signal fusion comprehensive data acquisition and analysis system, the synchronous acquisition of parameters such as pressure displacement, stress and strain of cylinder bearing, vehicle speed, load, and other parameters of oil and gas suspension cylinders is completed, to obtain real correlation test data for analysis and provide a basis for the development of oil and gas suspension systems.

## MATERIALS AND METHODS

### Mathematical Simulation of Oil and Gas Suspension Characteristics

The middle and rear suspension cylinders of the oil and gas suspension system structure are communicated through the accumulator and the hydraulic pipeline to form a hydraulic balanced suspension. So that the pressure of the connected suspension cylinder is always balanced and equal when the vehicle is driving on an uneven road surface because the suspension cylinder pipeline is connected, the leverage effect is formed, the oil in the cylinder is balanced when encountering obstacles, the dynamic force of each bridge suspension can be balanced, and the vertical load between the wheels of the same group of interconnection is evenly loaded, and the effective ground attachment of each wheel can be guaranteed. Avoid the impact of excessive impact load on the frame of the single axle (Zhang *et al.*, 2020).

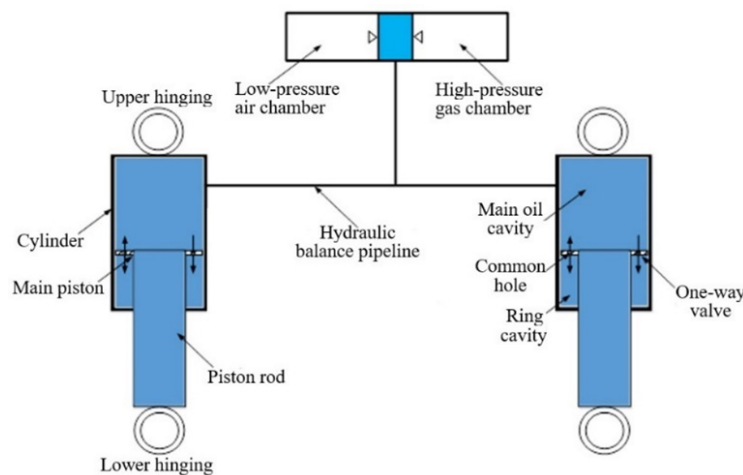


**Figure 1:** Hydraulic balanced oil and gas suspension structure diagram and principle

### Study on Elastic Characteristics of Oil and Gas Suspension

For the carrying vehicle, it is necessary to face different working conditions of no load and full load, so the double air chamber accumulator with high and low-pressure configuration is generally selected, and the elastic characteristics of oil and gas suspension need to be calculated in two stages, namely the working stage of the low-pressure air chamber and the joint working stage of the high-pressure air chamber and the low-pressure

air chamber. The working stage of the low-pressure air chamber corresponds to the no-load working condition, and the high-pressure air chamber and the low-pressure air chamber work together correspond to the full load working condition, so the working characteristics of the oil and gas suspension cylinder are affected by the pressure setting of the accumulator. The elastic characteristics of oil and gas suspension are divided into two stages, namely the no-load dynamic stroke working stage, and the full-load dynamic stroke stage (Ma *et al.*, 2003).

### The Working Stage of the Low-Pressure Air Chamber

When the oil and gas spring load is small, only the low-pressure gas chamber operates, and the gas pressure at any time in the low-pressure gas chamber is derived from the ideal gas equation of state (Li *et al.*, 2017).

$$P_L(i) = P_L \cdot (V_L / (V_L(i)))^m \quad (1)$$

Thereinto:

$V_L(i)$  — is the volume of gas in the low-pressure gas chamber at any given time;

$V_L$  — is the initial volume of the low-pressure air chamber;

$m$  — is the gas variability index;

$P_L$  — is the initial inflation pressure of the low-pressure air chamber;

$P_L(i)$  — is the value of the pressure change at any position when the low-pressure air chamber is operating.

The change in the volume of the low-pressure air chamber  $V_L(i)$  is due to a change in the strokes of the oil and gas spring.

$$V_L(i) = V_L - n \cdot A_g \cdot s \quad (2)$$

Thereinto:

$A_g$  — is the cross-sectional area of the piston rod;

$n$  — the number of balanced suspension cylinders;

$S$  — is the oil and gas spring stroke.

Simultaneous equations (1) and (2) give that the elastic

force of a single spring is:

$$F_{s1} = P_L(i) \cdot A_g = P_L \cdot (V_L / (V_L - n \cdot A_g \cdot s))^m \cdot A_g \quad (3)$$

### The Stage When the High-Pressure Air Chamber and The Low-Pressure Air Chamber Work Together

When the load of the oil and gas spring increases to the same as the load corresponding to the initial inflation pressure  $P_L$  of the high-pressure gas chamber, the low-pressure gas chamber and the high-pressure gas chamber begin to work together and the pressure is equal, and the critical volume of the low-pressure gas chamber is  $V_0$ , and the pressure of the high-pressure gas chamber and the low-pressure gas chamber working together at any time can be obtained from the ideal gas state equation of the low-pressure gas chamber is:

$$P_H(i) = P_H \cdot ((V_0 + V_H) / (V_0 + V_H - n \cdot A_g \cdot s))^m \quad (4)$$

The elastic force of a single spring is:

$$F_{s1} = P_H(i) \cdot A_g = P_H \cdot A_g \cdot ((V_0 + V_H) / (V_0 + V_H - n \cdot A_g \cdot s))^m \quad (5)$$

According to the derived analytical calculation formula, MATLAB was used to program. The suspension parameters were used as design inputs for simulation calculation, and the suspension characteristic curve was obtained, as shown in Figure 2-2.

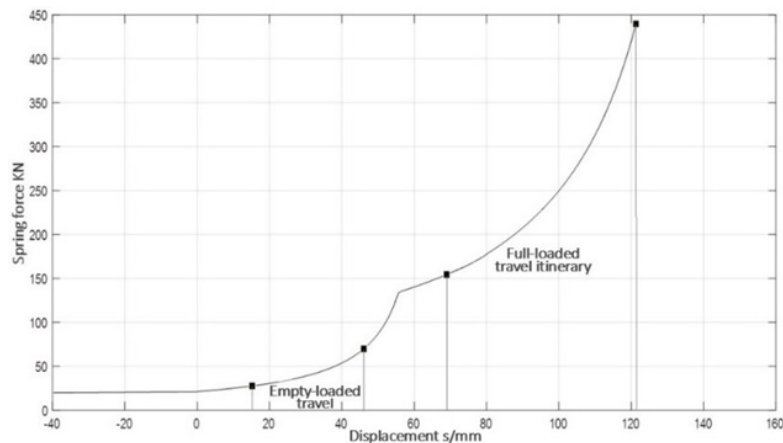


Figure 2: Characteristic curves of elastic forces in oil and gas suspension

### Simulation Analysis of Obstacle Crossing Performance of Balanced Oil and Gas Suspension

According to the structural characteristics of the balanced suspension and the hard point coordinates of the real vehicle suspension guide mechanism, a multi-body dynamic model of the oil and gas suspension system was

established, and the derived suspension characteristics were defined by spline curves to define the properties of the elastic elements in the simulation model, to realize the nonlinear characteristics of the balanced oil and gas suspension, and analyze the stroke change and output force of the balanced suspension cylinder (Cao *et al.*, 2011).

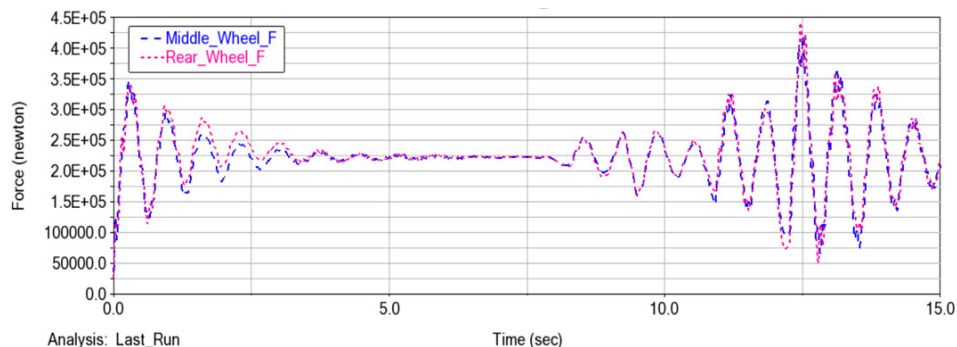


Figure 3: Calculation of the force of the suspension cylinder to calculate the change curve



### Simulation Analysis and Experimental Study of the Force of the Cylinder Bearing

The finite element analysis method is used to analyze the force of the cylinder bearing of the balanced suspension system, and the theoretical maximum position of the stress and strain of the cylinder support is obtained, which provides a theoretical basis for the strain gauge to arrange the measurement points.

#### Frame Finite Element Simulation Analysis

The frame of a certain type of three-axle rigid mincart adopts Q345D quenched and tempered steel (tensile strength: 450-630Mpa) in the support part of the oil and

gas suspension cylinder. In this paper, the frame force simulation analysis is carried out using Hyper mesh software for modeling, geometry cleaning, meshing, and solution settings, as well as Abaqus solver. The simulation calculates the obstacle and trench conditions used in Section 2.2 and applies boundary conditions and loads based on the results of mathematical simulations. The symmetrical boundary is applied according to the characteristics of the finite element model. The load time history of the actual working condition is determined. The obstacle crossing trench wheel applies a vertical upward concentrated force load, which is fully constrained except for the obstacle crossing trench wheel.

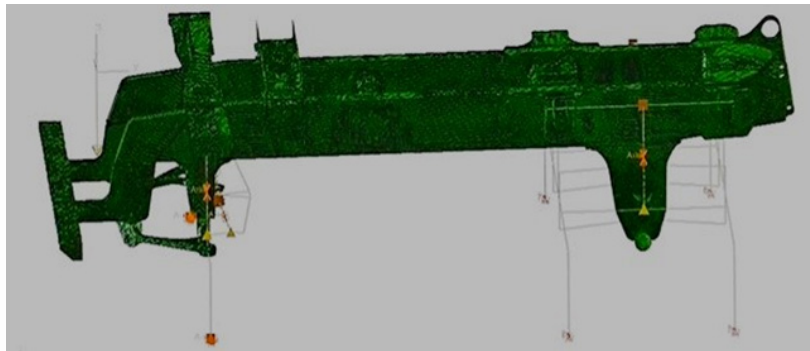


Figure 4: Finite element model of the frame

Through finite element solution, the Von Mises distribution cloud diagram is obtained, as shown in Figure 2-3. The location where the stress is concentrated is near the ear plate of the middle and rear suspension cylinders. According to the stress distribution cloud chart, when the rated load is 120%, the ultimate working condition is to cross the obstacle trench (depth 200mm), and the speed is greater than 25km/h, the maximum stress on both sides of the cylinder support plate can reach 260MPa, as shown in Figure 2-11 As shown, the stress displacement

range of normal driving is 160-190MPa.

According to the tensile strength of Q345D quenched and tempered steel: 450-630Mpa, during normal driving, the safety factor is about 3, and the minimum safety factor for crossing obstacle trenches is 1.73. Theoretically, the bigger the safety system, the better. If the frame strength is sufficient, it is the most economical way to improve the safety factor by optimizing the performance of the hydro-pneumatic suspension system.

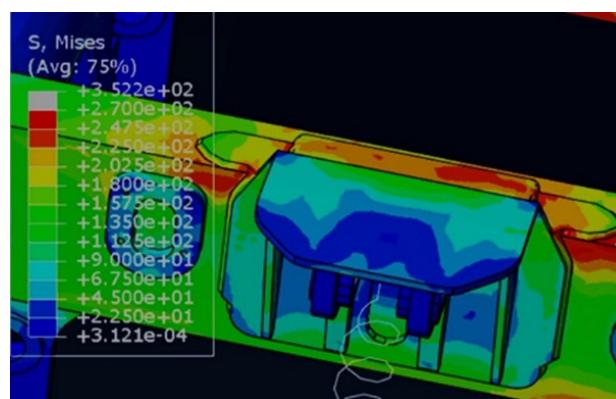


Figure 5: Partial stress distribution contour of cylinder support

#### Research on Strain Electric Method

As a structural part of the frame, when the mechanical test is carried out, the strain electric measurement method is generally used for testing. According to Hooke's law, the stress and strain of a material are linearly within a limited range, and the corresponding maximum stress is

called the proportional limit. The stress-to-strain ratio constant is known as the modulus of elasticity  $E$ , and every material has its inherent modulus of elasticity (Luo, 2008). Although the structural stress cannot be measured directly, the magnitude of the structural stress can be obtained by converting the structural stress-

strain relationship. The formula for the relationship between stress and strain is  $\sigma = E\epsilon$ , where  $\sigma$  is stress and  $\epsilon$  is strain. To calculate the stress of the strain gauge, it is also necessary to substitute the Poisson's ratio  $\mu = \epsilon_2/\epsilon_1$ , where  $\epsilon_1$  is the axial strain of the strain gauge and  $\epsilon_2$  is the transverse strain of the strain gauge (Zhang, 2006). For stress measurement points where the direction of the principal stress is unknown, the strain rosette can be used, and then the magnitude and direction of the principal

stress at the measurement point can be analyzed (Yang *et al.*, 2015). The working conditions of the mincart are complex, so each measuring point on the frame will not only be subjected to unidirectional stress, but each measuring point needs to be arranged with a strain gauge flower for testing (Luo *et al.*, 2021). In this paper, the most commonly used 45° right-angle strain gauge rosette is used, and the schematic diagram of the structure is shown in Figure 2-14.

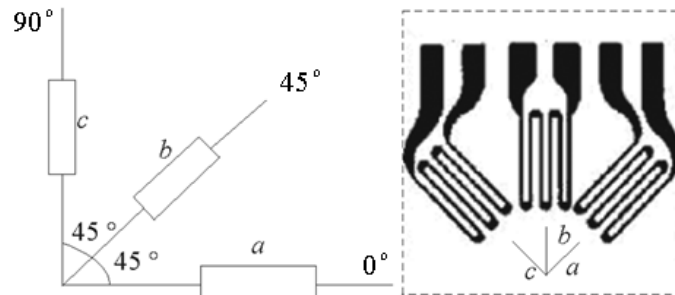


**Figure 6:** Schematic diagram of a 45° right-angle strain gauge rosette

The maximum principal stress and minimum principal stress of the 45° right-angle strain gauge rosette are respectively

$$\sigma_1 = \frac{E}{2(1-\mu)}(\epsilon_a + \epsilon_c) + \frac{E}{\sqrt{2}(1+\mu)}\sqrt{(\epsilon_a - \epsilon_b)^2 + (\epsilon_b - \epsilon_c)^2} \quad (6)$$

$$\sigma_2 = \frac{E}{2(1-\mu)}(\epsilon_a + \epsilon_c) - \frac{E}{\sqrt{2}(1+\mu)}\sqrt{(\epsilon_a - \epsilon_b)^2 + (\epsilon_b - \epsilon_c)^2} \quad (7)$$

Where  $\epsilon_a$  and  $\epsilon_c$  denotes the direction of strain in the three directions of 0°, 45°, and 90°, respectively.

The stress synthesis is carried out by using the fourth strength theory (Von Mises), and the equivalent stress is obtained  $\sigma$ :

$$\sigma = \sqrt{\frac{(\sigma_1 - \sigma_2)^2}{2} + \frac{(\sigma_2 - \sigma_3)^2}{2} + \frac{(\sigma_3 - \sigma_1)^2}{2}} \quad (8)$$

## RESULTS AND DISCUSSIONS

By building a multi-signal fusion comprehensive data acquisition and analysis system, and selecting appropriate sensors and acquisition modules, the synchronous acquisition of parameters such as suspension cylinder pressure displacement, stress and strain of cylinder support on the frame, vehicle speed, and load was completed, to obtain real test data for simulation model correction and oil and gas suspension system evaluation.

### Basic Information about Suspension Cylinders

**Table 1:** Suspension Cylinder Stroke Information

Working cylinder stroke	Stroke minimum/mm	Stroke maximum/mm
Front suspension cylinders	45	285
Medium suspension cylinders	5	205
Rear suspension cylinders	5	205

**Table 2:** Suspension Cylinder Stroke Information

Serial	Pilot project	Collection method	Sensor model
1	Load capacity, travel speed	CAN module	DEWE-43A
2	Road condition monitoring	GPS Module + camera	C270HB-WEB CAM
3	Front, middle, & rear suspension cylinder pressure	Pressure sensors	3403-18-C3.37
4	Front, middle, & rear suspension cylinder rod protrusion	Cable-type displacement sensor	MPS-M-1000-VT1K
5	Frame strain	45° Strain flowers	BE120-3CB(11)-Q30P300

### Sensor Placement

According to the acquisition scheme, the sensor is installed at the corresponding position of the three-axis rigid mincart, and auxiliary tools can be used.

### Installation of Cable-Type Displacement Sensor

To mitigate relative motion between the front suspension cylinder and its surrounding components during the steering process, a sliding mechanism is implemented.

This mechanism is affixed to the lower end of the cylinder rod. The displacement sensor, equipped with a cable, is connected to the sliding part, allowing the cable's free end to adjust automatically following the movement of the wire box. This design ensures that the cable

remains aligned parallel to the central axis of the cylinder, thereby ensuring that any variation in the length of the displacement sensor's cable directly corresponds to the actual extension or retraction of the cylinder rod (Zhang, 2023).

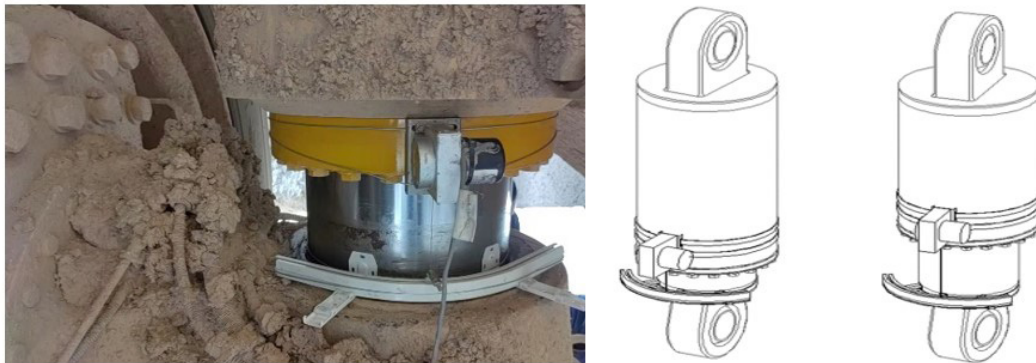


**Figure 7:** Cylinder mounting displacement (Sensor cable end automatically adjusts along the slide rail)

### High-Precision Pressure Sensor Installation

The pressure sensor can be installed by installing a

pressure measurement connection in the large cavity of the cylinder.

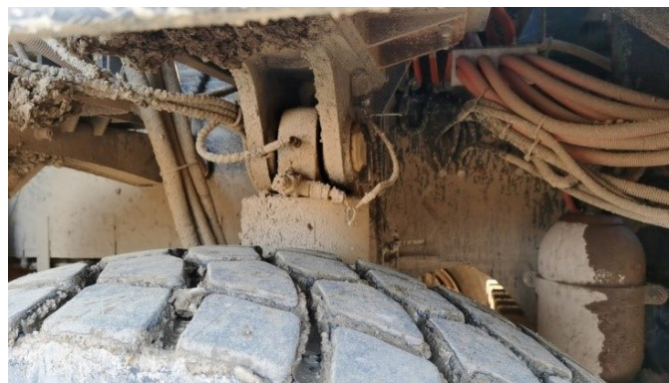


**Figure 8:** High-precision pressure sensor installed on a suspension cylinder

### Strain Gauge Installation

Based on the results of the finite element analysis, the strain gauges are arranged. As shown in Figure

3-3, the sampling frequency is set to 1000Hz, and the corresponding settings are completed in the software.

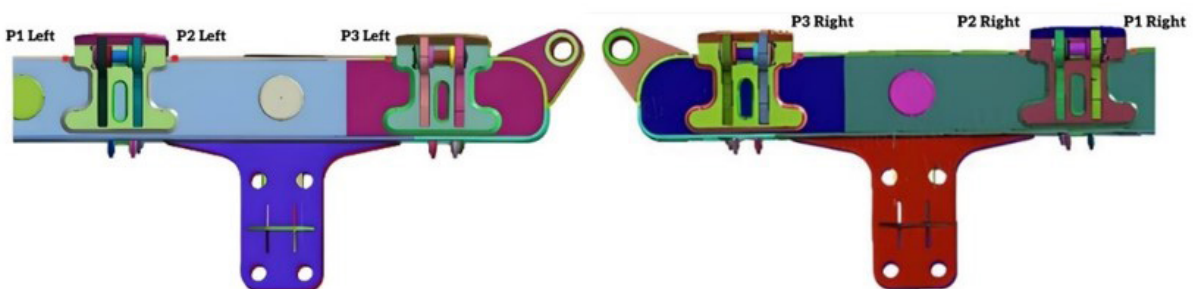


**Figure 9:** Schematic diagram of the installation of strain gauges on the middle and rear axle frames

### Performance Testing and Analysis of Oil and Gas Suspension System

The relationship between the force of the cylinder bearing on the frame and the characteristics of the cylinder was obtained by analysis, and the characteristics of the oil and gas suspension cylinder were evaluated by the driving smoothness index.

### Road Tests

To obtain comparable data with the simulation analysis, the 10km/h and 25km/h flat driving and obstacle crossing trench conditions were designed, and the obstacle height and trench depth were both 200 mm (determined according to the total stroke of the middle and rear suspension cylinders). To better reflect the



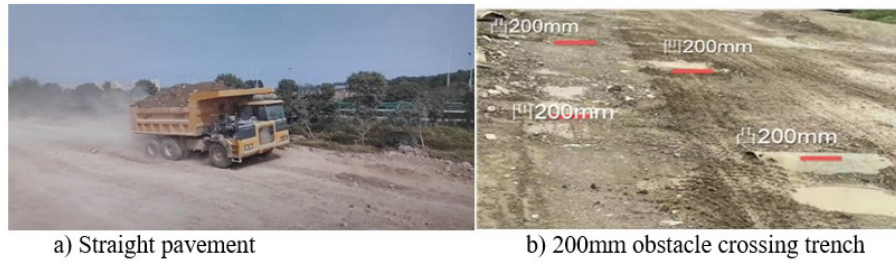


**Figure 10:** Schematic diagram of traffic settings

full-stroke adjustment performance of the cylinder, the loading capacity is increased to the maximum allowable overload, i.e., overload by 20%.

### Static Tests

Before the dynamic test, the initial parameter information collection and status confirmation of the oil and gas suspension system should be carried out.

### No-Load Initial Parameters

Place the vehicle on a flat road with no load, and observe the pressure, height adjustment, and stability of the suspension system. Check the vehicle's balance and the accuracy of suspension height adjustment.

### Initial Parameters of Full Load

After the vehicle is loaded, it is placed on a flat road surface to observe the pressure, height adjustment, and stability of the suspension system. Check the adaptive performance of the vehicle's suspension system when the load changes.

Before the stress-strain test of the cylinder bearing, the initial value of the strain should be calibrated. After the cargo box of the vehicle is lifted, the installation of the strain gauge is completed first, and after the cargo box is

put down, the vehicle is placed on a flat road surface to carry out the strain zeroing treatment.

### Dynamic Tests

During the dynamic test, the changes in the acquisition curve were observed, and the abnormal response was found to eliminate the problem and the acquisition was re-collected. Under the condition of no and full load, the signal acquisition under different working conditions is carried out:

### Test of Working Characteristics of Oil and Gas Suspension Cylinder

Collect the displacement and pressure value changes of oil and gas suspension cylinders. It is used to evaluate the stiffness characteristics and responsiveness of suspension systems.

### Cylinder Bearing Stress and Strain Test

collect the stress change of the cylinder bearing. It is used to analyze the influence of oil and gas suspension stiffness change on the stress and strain of cylinder bearings.

### Test Results of Oil and Gas Suspension Cylinders

From the pressure curve trend analysis:

The spring characteristics of the front suspension cylinder

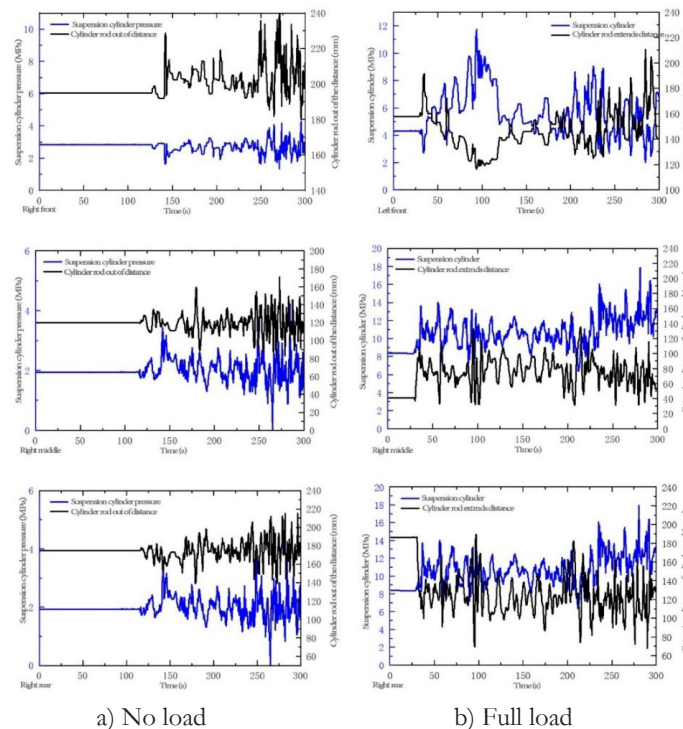


**Figure 11:** Pressure and displacement changes in the trench section of the suspension cylinder



are very obvious, and the pressure and displacement show an obvious inverse proportional relationship. Although the middle and rear suspension also show a certain inverse proportional relationship, there is also an uncoordinated situation, that is, the pressure of the suspension cylinder is increased but the displacement is inconsistent, the reason for this situation should be that the middle and rear suspension cylinders are directly connected with the accumulator, and the phenomenon that the middle and rear suspension cylinders are restrained by each other.

### Analysis of the Relationship between Suspension Cylinder Pressure and Protrusion

By analyzing the relationship between the pressure of the suspension cylinder and the amount of extension, the stiffness characteristics of the front suspension cylinder and the accumulator characteristics are verified:

### Front Suspension Cylinder Pressure

after the data is cleaned, the scatter plot of the pressure and protrusion of the front suspension cylinder in the no-load and full-load state is drawn (Fig. 4-2), the graph shows obvious mathematical characteristics, and the 6-level polynomial formula is obtained by fitting the curve, which can be substituted into the mathematical model to check the cylinder stiffness characteristics.

### Accumulator Parameters

after the data is cleaned, the scatter plot of the pressure and extension of the middle and rear suspension cylinders in the full load and no-load states is drawn (Fig. 4-3), and there are obvious working areas in the no-load and full-load states, which reflects the characteristics of the low pressure and high-pressure working areas of the accumulator.

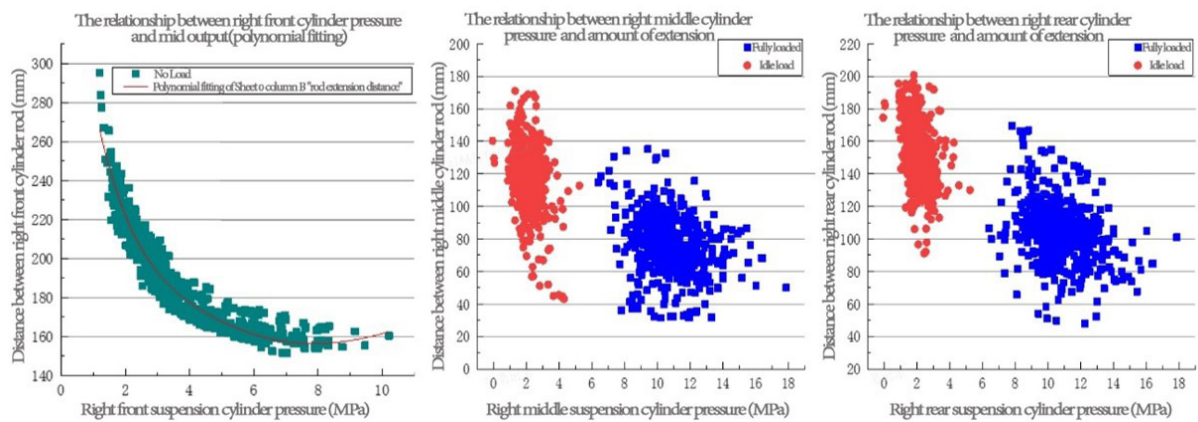


Figure 12: Relationship between cylinder pressure extension and pressure

### Mises Stress Analysis at the Measurement Point

The time-domain signal curve of the strain gauge generated by the strain gauge during the operation of the frame can be obtained through the acquisition software, and the Mises stress value of the strain gauge at each test position can be obtained through the analysis function of the acquisition software.

Select the loading stress and time curve diagram of the left and right P1 and P2 measuring points, the stress value of the measuring point increases with the increase of load, and the impact generated by the loaded material can be recorded from the curve, and the loading stops loading at 120% full load.

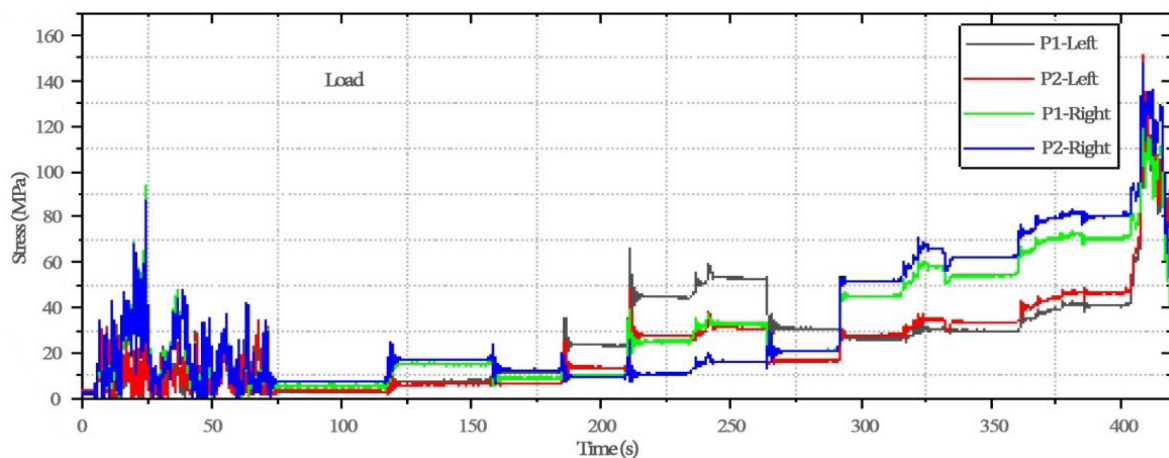
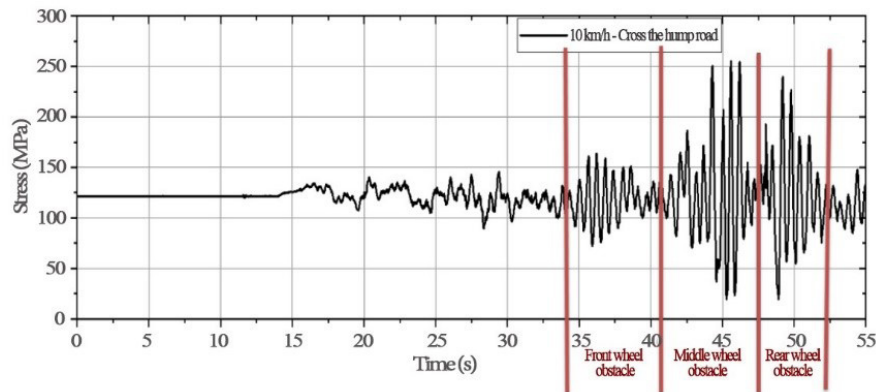


Figure 13: Stress changes during loading of the left PI measuring point

## Analysis of Cylinder Support Stress and Cylinder Displacement

Take the stress and time curve of the high-stress left P1 measuring point at a constant speed of 10km/h over an obstacle trench (Figure 14), combined with

the displacement time curves of the left front, middle, and rear overhang of the vehicle at a constant speed of 10km/h over the obstacle trench (Figure 15) It can be found that high stress occurs in the middle wheel and rear wheel during obstacle crossing.



**Figure 14:** Stress variation and time curve of the 10km/h uniform speed obstacle crossing trench at the left P1 measuring point

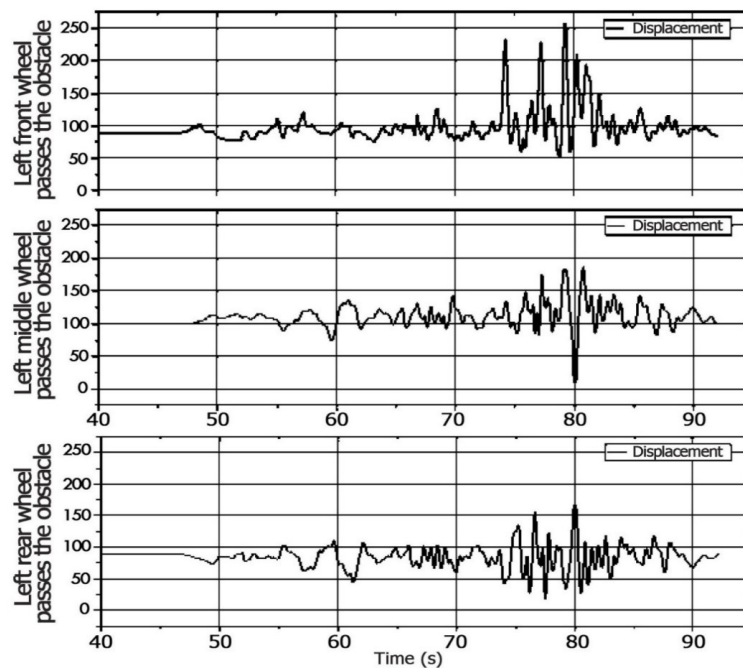


**Figure 15:** Displacement time curves of the left front, middle, and rear overhangs of the trench crossing at a constant speed with a load of 10km/h

## RESULTS AND DISCUSSION

This research revealed significant findings regarding the dynamic performance and stress distribution of the oil and gas suspension system:

### Elastic Characteristics

Nonlinear stiffness was observed across both low-pressure and high-pressure working stages. Simulation results validated the elasticity model, showing close alignment with polynomial stiffness curves.

The transition between low and high-pressure chambers impacts suspension stiffness, particularly under heavy loads.

### Trench-Crossing Analysis

The front suspension exhibited predictable pressure-displacement relationships, while inconsistencies were noted in middle and rear suspensions due to inter-cylinder interactions via shared accumulators.

Stress concentration occurred at cylinder support plates, with maximum stress levels nearing the material's safety limits under extreme conditions.

### Cylinder Force Dynamics

The analysis confirmed that the pressure and displacement of cylinders are inversely proportional, with deviations attributed to structural design limitations in hydraulic balancing.

## Road Testing

Full-load tests demonstrated that increased suspension stiffness leads to higher stress levels in frame supports. Strain gauge data provided quantitative evidence, revealing stress peaks during trench crossings.

These findings highlight the need for refined accumulator configurations and reinforced frame materials to enhance durability and responsiveness under dynamic conditions.

## CONCLUSION

The analysis of the nonlinear characteristics of the hydro-pneumatic suspension system in a three-axle rigid mine car reveals critical insights into its operational dynamics. The findings, particularly concerning the inverse relationship between pressure and displacement within the suspension cylinders, emphasize the intricacy of the interactions among suspension components during varying loading conditions. The identified high-stress concentrations at pivotal points further underscore the necessity for targeted improvements to enhance the durability and performance of the suspension system.

## RECOMMENDATION

Future research opportunities abound in deepening our understanding of suspension dynamics by incorporating advanced materials, such as composites, to investigate their impact on weight reduction and overall suspension performance. Additionally, real-time monitoring systems could be integrated to analyze instantaneous responses during various driving conditions, offering rich datasets for machine learning algorithms to optimize suspension settings dynamically.

## REFERENCES

- Cao, R. Y., Zhang, H., & Xiong, S. B. (2011). Modeling and simulation of hydro-pneumatic suspension of mine truck. *Machinery Design & Manufacture*, (1), 239-241.
- Design and performance research of a hydro-pneumatic suspension with variable damping and stiffness characteristics. *Journal of Mechanical Science and Technology*, 36, 4913-4923. <https://doi.org/10.1007/s12206-022-0905-0>
- Dong, L., & Cui, M. (2021). Fatigue life analysis and optimization of three-bridge rigid minecart frame. *Automation Application*, 1, 138-140.
- Fei, J. P. (2015). Simulation on pressure characteristic of hydro-pneumatic suspension with single-acting cylinder. *Manufacturing Automation*, 3, 59-61.
- Feng, S., & Wang, G. (2000). Current status and development of oil-gas suspension for engineering vehicles. *Mining Machinery*, 28(12), 32-33. [https://lib.cqvip.com/Qikan/Article/Detail?id=4956146&from=Qikan\\_Article\\_Detail](https://lib.cqvip.com/Qikan/Article/Detail?id=4956146&from=Qikan_Article_Detail)
- Goodall, R. M., & Kortüm, W. (1983). Active controls in ground transportation: A review of the state-of-the-art and future potential. *Vehicle System Dynamics*, 12(4-5), 225-257. <https://doi.org/10.1080/00423118308968755>
- Guan, Q., Gong, A., Hu, M., Liao, Z., & Chen, X. (2021). Anti-rollover warning control of dump truck lifting operation based on active suspension. *Journal of Control, Automation and Electrical Systems*, 32, 109-119. <https://doi.org/10.1007/s40313-020-00664-y>
- Guo, K. (2021). Performance analysis of multi-load mode suspension system of heavy engineering vehicles. *Construction Machinery*, 8, 19-22.
- Li, R. (2015). *Research on drive axle design and dynamic characteristics of electric wheel mining dump truck* (Master's thesis). University of Science and Technology Beijing.
- Li, Z., Guo, Z., Wang, C., Li, M., & Ma, Z. (2017). Modeling and simulating of a two-stage pressure hydro-pneumatic spring for off-road vehicles. *Zhendong Ceshi Yu Zhenyuan/Journal of Vibration, Measurement and Diagnosis*, 37, 512-517. <https://doi.org/10.16450/j.cnki.issn.1004-6801.2017.03.015>
- Luo, K., Yuan, W., & Si, M. (2021). Fatigue life estimation of dump truck frame structure based on road test. *Journal of Qingdao University: Engineering Technology Edition*, (4), 101-106.
- Luo, P. (2008). The innovation of Hooke's Law and the creation and development of "strength stability comprehensive theory. *Journal of Harbin Engineering University*, 29(7), 10.
- Ma, G., Wang, S., & Tan, R. (2003). Research on mathematical model and computer simulation of automobile oil-gas suspension system. *China Mechanical Engineering*, 14(11), 978-981. [https://qikan.cqvip.com/Qikan/Article/Detail?id=7859137&from=Qikan\\_Article\\_Detail](https://qikan.cqvip.com/Qikan/Article/Detail?id=7859137&from=Qikan_Article_Detail)
- Margolis, D. L. (1983). Semi-active control of wheel hop in ground vehicles. *Vehicle System Dynamics*, 12(6), 317-330. <https://doi.org/10.1080/00423118308968760>
- Wang, S., Li, X., Zhang, L., & Bian, J. (2021). Study on the property rights system of mineral resources in China. *China Mining Magazine*, 30(9), 16-19. <https://doi.org/10.12075/j.issn.1004-4051.2021.09.029>
- Wu, W., Tang, H., Zhang, S. (2020). High-precision dynamics characteristic modeling method research considering the influence factors of hydropneumatic suspension. *Shock and Vibration*, 2020, 1-21. <https://doi.org/10.1155/2020/8886631>
- Yang, J. (2015). Stress monitoring system for oil pipeline based on right-angle strain gauge rosette. *Ordance Industry Automation*, (3), 74-76.
- Zhang, H. (2006). Analysis on strain measurement and data processing methods under complex stress conditions. *China Testing Technology*, (2), 52-55.
- Zhang, L. (2013). *Optimization design of oil and gas suspension based on ride comfort* (Master's thesis). Hunan University.
- Zhang, Y. (2023). A measuring device for the extension of oil cylinder. *Patent No. 202322523172*.
- Zhang, Y., Dong, L., Han, X., Xu, M., & He, L. (2020, October). Simulation Analysis and Test of Hydraulic Balanced Oil-gas Suspension Crossing Performance. In *2020 9th International Conference on Power Science and*

*Engineering (ICPSE)* (pp. 48-51). IEEE. <https://doi.org/10.1109/ICPSE51196.2020.9354364>  
Zhu, G. (2009). Suggestions on the efficient development

and utilization of solid mineral resources in the  
“Twelfth Five-Year Plan” large-scale mining electric  
wheel dump trucks. *Electrical Abstracts*, (002), 70-73.